Nat Neurosci. Author manuscript; available in PMC 2016 April 25.

Published in final edited form as:

Nat Neurosci. 2013 May ; 16(5): 596–604. doi:10.1038/nn.3374.

Glucocorticoid feedback uncovers retrograde opioid signaling at hypothalamic synapses

Jaclyn I. Wamsteeker Cusulin[*], **Tamás Füzesi**[*], **Wataru Inoue**[*], and **Jaideep S. Bains**[*,#]

[*]Hotchkiss Brain Institute & Dept. of Physiology and Pharmacology, University of Calgary, 3330 Hospital Dr. NW, Calgary, Alberta, T2N 4N1, Canada

Abstract

Stressful experience initiates a neuroendocrine response culminating in the release of glucocorticoid hormones into the blood. Glucocorticoids feed back to the brain causing adaptations that prevent excessive hormone responses to subsequent challenges. How these changes occur remains unknown. We report that glucocorticoid receptor activation in rodent hypothalamic neuroendocrine neurons following *in vivo* stress is a metaplastic signal that allows GABA synapses to undergo activity–dependent long–term depression (LTD_{GABA}). LTD_{GABA} is unmasked through glucocorticoid receptor inhibition of Regulator of G–protein Signaling 4 (RGS4), which amplifies signaling through postsynaptic metabotropic glutamate receptors (mGluRs). This drives somatodendritic opioid release, resulting in a persistent retrograde suppression of synaptic transmission through presynaptic μ–receptors. Together our data provide new evidence for retrograde opioid signaling at synapses in neuroendocrine circuits and represent a potential mechanism underlying GC contributions to stress adaptation.

Exposure to stress results in two prominent hormonal responses: central and peripheral catecholamine release and a surge of glucocorticoids into the blood stream. Through temporally and mechanistically distinct pathways, both mediators are essential for appropriate behavior and mood regulation[1,2]. One unique and critical function of glucocorticoids on stress circuits is that they feedback to curtail hormone release in response to subsequent challenges. This serves a self-limiting homeostatic function in the face of diverse and repeated stress challenges[3]. Despite this fundamental role for glucocorticoids in shaping endocrine function with experience, relatively little is known about how it might be accomplished.

Adaptive control of the neuroendocrine response to stress resides with a small cluster of neurons in the paraventricular nucleus of the hypothalamus (PVN). These parvocellular neuroendocrine cells (PNCs) at the head of the hypothalamic-pituitary-adrenal (HPA)/stress-

[#]Corresponding author: Telephone: 1 (403) 220 7585, Fax: 1 (403) 283 2700, jsbains@ucalgary.ca.

Author Contributions

J.I.W designed and conducted experiments, analyzed the data and wrote the manuscript. T.F. and W.I. conducted experiments, analyzed data, and contributed to manuscript preparation. J.S.B. designed experiments, prepared the manuscript and supervised the project.

axis are positioned as the definitive point of neural stress integration; their activity is a function of both synaptic drive and negative feedback by glucocorticoids[3]. The dominant share of synapses onto PNCs are GABAergic[4]. GABA transmission onto PNCs restrains basal stress axis output[5] and is, itself, sensitive to stress[6,7]. Importantly, stress exposure causes diminished chloride extrusion capacity in PNCs, resulting in a situation in which GABA is excitatory during stress[5,8]. Thus, although it is counterintuitive, dampening GABA transmission alleviates the activation of the endocrine response[8].

In addition to corticotropin-releasing hormone (CRH) and vasopressin, PNCs synthesize proenkephalin-derived opioid peptides[9]. Enkephalins have been implicated as putative mediators of adaptive change to stress-axis function[9]. Consistent with this idea, mice lacking proenkephalin exhibit prolonged GC elevation to stress[10], suggesting opioids may participate in GC negative feedback. The cellular actions of endogenous opioid signaling have not been explored in PNCs; in other systems, they function as retrograde signals to inhibit neurotransmitter release[11,12]. We hypothesized that opioids are intermediaries of glucocorticoid actions in the PVN. Using whole-cell patch-clamp recordings of PNCs from naïve and stress-exposed rats, we examined GABA synapse strength and responses to patterned afferent activity. We report that a single stressful experience, followed by a 90-min temporal delay unmasks activity-dependent, heterosynaptic long-term depression of GABA (LTD_{GABA}) synapses that is mediated by retrograde opioid signaling.

Results

Glucocorticoid receptor activation during stress unmasks LTD_{GABA}

In response to an acute stress, plasma corticosterone (CORT, the major rodent glucocorticoid) rapidly rises; peak concentrations are reached 15–30 min from stress onset, persist during the stress, and subside slowly thereafter[1]. Subsequent access of CORT to the brain is regulated and time of peak elevation lags that of plasma CORT[13]. To investigate potential effects of CORT exposure resulting from stress, we examined PNCs in *in vitro* hypothalamic slices prepared from rats exposed to 30 min of immobilization stress followed by incrementally increasing periods of recovery before sacrifice (Fig. 1a). Naïve (unstressed) rats served as our age-matched controls. In whole-cell voltage-clamp recordings at −80 mV, we electrically evoked inhibitory postsynaptic currents (eIPSCs; in 10 μM DNQX)). eIPSC amplitude was used as an indicator of synaptic strength. We did not observe any significant alterations in cellular or synaptic properties between cells obtained from naïve (n = 142) versus stressed (n = 40) animals (Supplementary Fig. 1). Following 10 min baseline recording, we paired afferent, 10-Hz synaptic stimulation with subthreshold depolarization to −40 mV for 5 min: a protocol reminiscent of those used at various synapses to induce activity-dependent plasticity[14,15]. In naïve slices, pairing transiently suppressed of eIPSC amplitude (84.9 ± 6.6% baseline amplitude; Fig. 1b), which recovered quickly (104.4 ± 4.5% baseline at 30 min, Fig. 1b). Pairing in slices prepared immediately following the stress potentiated of eIPSCs (LTP: to 126.6 ± 10.2% baseline at 30 min one-sample t-test P = 0.039; Fig. 1c), similar to that observed by Inoue et al. (see accompanying paper). In slices from animals allowed to recover 30 or 60 min following the end of stress, we failed to observe any persistent changes to eIPSC amplitude (Fig. 1d–e). Further extending the post-

stress recovery period to 90 min produced both an initial depression (42.4 ± 5.2%; P < 0.0001; Fig. 1f) and unmasked a long-term depression of eIPSC amplitude (LTD_{GABA}) that persisted at least 30 min after pairing (69.4 ± 8.3% baseline; P = 0.0042). LTD_{GABA} was not evident in naïve slices when pairing protocol duration was increased (92.7 ± 5.6%; P = 0.24; Supplementary Fig. 2f), suggesting that a threshold change does not underlie differences in responses between naïve and stressed rats. These results demonstrate that acute stress, with varied temporal delay, uncovers both conditional activity-dependent LTP and LTD_{GABA} in PNCs.

The temporal delay in unmasking of LTD_{GABA} following acute immobilization is consistent with exposure to an *in vivo* associative signal, like CORT, which canonically has a slow onset of action compared with noradrenaline[2]. Consequently we tested whether activation of glucocorticoid receptors is an obligatory permissive factor for LTD_{GABA}. Animals were given an intraperitoneal injection of either the glucocorticoid receptor antagonist RU-486 (25 $mg \cdot kg^{-1}$) or vehicle (DMSO) 15 min prior to immobilization and allowed to recover for 90 min afterwards (Fig. 2a). I*n vivo* RU-486 pre-treatment completely prevented LTD_{GABA} (102.9 ± 5.0% baseline; P = 0.58; Fig. 2b). Vehicle injection had no effect (67.8 ± 8.1% baseline; P < 0.0001). These data demonstrate that glucocorticoid receptor activation is necessary for stress-associated LTD_{GABA}. They do not, however, provide information about anatomical specificity, nor do they indicate whether glucocorticoid receptor activation is sufficient in the absence of stress. Thus our next experiments probed the actions of local CORT administration to *in vitro* hypothalamic slices. Individual slices from naïve rats were incubated in CORT (100 nM) either with or without RU-486 (500 nM) for one hour followed by an additional 30-min recovery period prior to recording (Fig. 2c). As with stress, we did not observe any changes in basal cellular and synaptic properties in CORT-treated PNCs (Supplementary Fig. 1). We did observe LTD_{GABA} in response to pairing in CORT-exposed cells (69.4 ± 4.9 % baseline; P < 0.0001; Fig. 2d). These changes were prevented by co-incubation with RU-486 (104.3 ± 5.5% baseline; P = 0.46). Next, we asked whether other stressors, which activate the HPA axis and elevate CORT, could also unmask LTD_{GABA}. We observed LTD_{GABA} in response to pairing in slices obtained 90 min following either forced swim or predator odor exposure (swim: 66.6 ± 9.2 % and predator: 73.8 ± 7.0 % baseline; P = 0.015 and P = 0.020; Fig. 2e–f). Together, these findings indicate that local glucocorticoid receptor activation in PNCs following stressful experience is necessary and sufficient to permit the induction of activity-dependent LTD_{GABA}.

We next probed for a locus (presynaptic vs. postsynaptic) of expression for LTD_{GABA}. To assess GABA release probability (p_r) during these experiments, we examined variability in eIPSC amplitude (inverse squared coefficient of variation: CV^{-2}) and the ratio between a pair of eIPSCs delivered in brief succession (paired-pulse ratio: PPR). 30 min after pairing, CV^{-2} was reduced in stressed cells (to 59.7 ± 10.8% baseline; P = 0.004; Fig. 3c), but remained unchanged in naïve cells (118.3 ± 15.2% baseline; P = 0.26). PPR was unchanged by pairing in naïve cells (99.8 ± 4.7% baseline; P = 0.97; Fig. 3d), but it was significantly increased in stressed cells (118.2 ± 6.8 % baseline, P = 0.021; from 0.62 ± 0.14 to 0.75 ± 0.21 un-normalized PPR; P = 0.009 paired t-test). Next we analyzed the inter-event interval/frequency and amplitude of spontaneous IPSCs (sIPSCs) from these recordings (Fig. 3e–g). sIPSC frequency decreased in cells from stressed (74.7 ± 4.6% baseline; P <

0.0001; Fig. 3e–f) but not naïve animals (106.9 ± 9.0% baseline; P = 0.46). sIPSC amplitude remained unchanged in both conditions (Fig. 3g). These data are consistent with decreased presynaptic release during LTD_{GABA}. Similarly, we noted that LTD in CORT treated slices was also accompanied by an increase in PPR (to 119.2 ± 6.5% baseline; P = 0.010; Supplementary Fig. 2a), a decrease in CV^{-2} (62.7 ± 7.4% baseline; P = 0.0002; Fig. 3h), and a reduction in sIPSC frequency, but not amplitude (frequency to 77.5 ± 6.9% baseline; P = 0.016; Supplementary Fig. 2b–e). Indeed, across *in vivo* and *in vitro* experimental conditions, changes to CV^{-2} were consistently related to changes in eIPSC amplitude (Fig. 3h). Taken together, our data strongly indicate that glucocorticoid-associated LTD_{GABA} is a consequence of a decrease in presynaptic GABA p_r.

LTD_{GABA} is induced heterosynaptically

Since electrical stimulation of synaptic inputs could recruit axons non-specifically, we used an optogenetic tool to test whether exclusive activation of GABA synapses was sufficient for LTD induction. Using CORT-treated slices from *vGAT–mhChR2–YFP* mice expressing channelrhodopsin under the vesicular GABA transporter promoter, we found that pairing delivered with light-evoked stimulation did not elicit LTD_{GABA}, while electrical stimulation in wild-type mice did(ChR2: 119.6 ± 12.3% baseline, electrical: 74.5 ± 5.8% baseline; P = 0.17 and P = 0.003 respectively; Fig. 4a).

Metabotropic glutamate receptors (mGluRs) are important for GABA synapse plasticity requiring heterosynaptic induction[14–16]. We conducted experiments to test for the mGluR contributions in LTD_{GABA}. In CORT treated slices we failed to induce LTD_{GABA} in the presence of the non-selective group I/II mGluR antagonist MCPG (200 μM, 97.9 ± 7.5% baseline; P = 0.93; Supplementary Fig. 3a). We next tested group I mGluR subtypes 1 and 5. Treatment with $mGluR_5$ antagonist MTEP (10 μM) completely abolished LTD_{GABA} in CORT treated slices (eIPSC: 101.0 ± 5.0% baseline; n = 5; P = 0.84; Fig. 4b). By contrast, inclusion of selective $mGluR_1$ antagonist JNJ-16259685 (750 nM) did not prevent LTD_{GABA} (73.2 ± 7.6% baseline; P = 0.017; Fig. 4c). Preventing activation of NMDA receptors with intracellular MK801 (1 mM) also failed to impact the expression of LTD_{GABA} (73.6 ± 5.0% baseline; P = 0.006; Supplementary Fig. 3b). These data indicate that group I mGluRs, in particular $mGluR_5$, are part of a heterosynaptic mechanism involved in LTD_{GABA} following GC exposure.

A postsynaptic, vesicle-based retrograde signal mediates LTD_{GABA}—We next tested whether the mGluR responsible for induction of LTD_{GABA} is postsynaptic. We interfered with G-protein signaling only in the postsynaptic PNC by including the non-hydrolysable GDP analogue GDPβs (2 mM) in the intrapipette solution. Under these conditions we failed to observe LTD_{GABA} in CORT treated cells (104.8 ± 7.7% baseline; P = 0.56; Fig. 4d). Since $mGluR_5$ is coupled to $G_{\alpha q}$–type intracellular pathways and exerts many effects through elevations in intracellular calcium, we next assessed the effect of fast calcium buffer BAPTA (10 mM), also intrapipette. This, too, prevented expression of LTD_{GABA} (102.0 ± 8.1% baseline; P = 0.81; Fig. 4e). Since postsynaptic depolarization was necessary LTD_{GABA} induction, we tested the involvement of voltage-dependent calcium channels. Consistent with this idea, the L-type calcium channel antagonist nimodipine prevented

LTD_{GABA} (99.5 ± 12.3 % baseline; P = 0.97; Fig. 4g). These results provide evidence that a post-synaptic mGluR- and calcium-dependent signaling pathway is required for LTD_{GABA} following CORT exposure.

LTD_{GABA} requires heterosynaptic activation of postsynaptic $mGluR_5$, but manifests as a presynaptic decrease in release probability, suggesting the presence of a retrograde signal. One widely described form of mGluR-dependent LTD_{GABA} requires retrograde signaling by endocannabinoids (eCBs)[16–18]. We have previously characterized short-term retrograde eCB signaling at GABA synapses onto PNCs[7] indicating that eCBs are functional at these synapses; since we found that short-term eCB signaling is enhanced by acute exposure to CORT, we hypothesized that recruitment of eCBs and activation of CB1Rs may contribute to GC-LTD_{GABA}. Following exposure to CORT, slices were incubated in aCSF containing CB1R antagonist AM251 (3 μM), for a minimum of 30 min. CB1R blockade, however, failed to prevent LTD_{GABA} (72.6 ± 3.2 % baseline; P < 0.0001; Fig. 4g). To further test this idea, we using genetic deletion assessing LTD_{GABA} in mice lacking CB1Rs (*CB1R*$^{-/-}$). We found that that LTD_{GABA} persisted in CORT treated slices from *CB1R*$^{-/-}$ mice (72.7 ± 5.1 % baseline; P = 0.0032; Fig. 4h). A TRPV antagonist, capsazepine, also failed to prevent LTD_{GABA} (66.4 ± 8.5 % baseline; P = 0.016; Supplementary Fig. 3c). Based on these data, we conclude that eCBs are not the retrograde signal responsible for expression of LTD_{GABA} at these synapses.

In addition to lipid-derived retrograde messengers, neurons, including PNCs[19], also release conventional and peptide transmitters that are packaged in vesicles in the somatodendritic compartment[17]. To test for the contribution of a vesicularly packaged retrograde transmitter, we conducted experiments in which the soluble NSF attachment protein receptor (SNARE)-dependent exocytosis inhibitor botulinum toxin C (BoNT/C: 5 μg·ml^{-1}) was included in the patch pipette. Inclusion of BoNT/C prevented LTD_{GABA} following pairing (105.3 ± 7.0% baseline; P = 0.49; Fig. 4i). Collectively, these observations indicate that LTD_{GABA} requires activation of postsynaptic mGluRs, an increase in intracellular calcium and the fusion of neurotransmitter-filled vesicles postsynaptically. Given that these events underlie presynaptic reduction of GABA release, a retrograde signal is likely recruited by this mechanism.

Glucocorticoids alter mGluR signaling via RGS4

We next tested whether pharmacological activation of mGluRs was sufficient to recapitulate suppression of GABA transmission, and whether this mechanism was altered by glucocorticoid exposure. As LTD_{GABA} requires high voltage activated L-type calcium channels and is evident only when afferent stimulation and depolarization to −40 mV are paired together (Depol. Alone: 118.3 ± 10.8% baseline, P = 0.15; Stim. Alone: 92.6 ± 6.8% baseline, P = 0.31; Supplementary Fig. 2g–h), we tested the hypothesis that LTD_{GABA} results from membrane state-dependent activation of mGluRs. We performed recordings of eIPSCs at either −40 mV, or −80 mV and bath-applied the group I mGluR agonist DHPG (100 μM) for 5 min. At −40 mV eIPSCs are outward currents; we lowered intracellular chloride (4 mM) to increase the inward driving force through the $GABA_A$ receptor. We first confirmed that LTD_{GABA} was still readily observed with reversed chloride driving force

(70.4 ± 9.2% baseline; P = 0.02; Supplementary Fig. 2i). Surprisingly, DHPG potentiated eIPSC amplitude in naïve slices under these conditions (132.3 ± 11.6% baseline at 10 min; P = 0.049; Fig. 5a). By contrast, in CORT-treated slices, DHPG elicited long lasting depression of eIPSCs (63.0 ± 4.7 % baseline; P = 0.0006; Fig. 5a), which was accompanied by increased PPR (119.6 ± 2.7% baseline; P = 0.0020; Fig. 5b) and a decrease in eIPSC CV $^{-2}$ (49.5 ± 7.6% baseline; P = 0.0012; Fig. 5b). Similar results were obtained at −80 mV; following CORT treatment DHPG no longer enhanced eIPSC amplitude, as it did in naïve cells, although no significant depression was observed (76.6 ± 10.6% baseline; P = 0.069; Supplementary Fig. 2k). From these data we conclude that mGluR activation, at a depolarized membrane potential is sufficient to recapitulate LTD_{GABA}. Furthermore, CORT exposure unmasks LTD_{GABA} by functionally altering the outcome of mGluR signaling.

We next sought to examine how glucorticoids alter mGluR signaling. Regulator of G-protein signaling (RGS) proteins, in particular RGS4, associate with group I mGluRs and stifle G_q mediated signaling through GTP-ase acceleration[20]. RGS4 is abundantly expressed in the PVN and potently down-regulated by stress/glucocorticoid receptor activation[21,22]; this provides a compelling and testable potential mechanism. To test the hypothesis that RGS4 restrains mGluR signaling in naïve PNCs, we included the RGS4 inhibitor CCG63802 (100 μM) in the pipette solution and bath applied DHPG. Postsynaptic inhibition of RGS4 was sufficient to unmask a DHPG-mediated LTD_{GABA} that was similar to that seen with CORT treatment (to 71.2 ± 7.0 % baseline; P = 0.0093; Fig. 5c). We next conducted the corollary experiment and included recombinant RGS4 in the patch pipette when recording from cells in CORT-treated slices. This completely prevented eIPSC depression following DHPG (132.0 ± 11.3 %; P = 0.036; Fig. 5d). These data indicate that RGS4 downregulation by glucocortioids is sufficient to enhance $mGluR_5$ signaling and allow for the expression of LTD.

Persistent μ-opioid receptor signaling underlies LTD_{GABA}

PVN neuroendocrine cells release neurotransmitters from vesicles in their somatodendritic compartment[19,23]. Opioid peptides released from magnocellular neurosecretory cells (MNCs) cause presynaptic LTD at glutamate synapses[11,24]. PNCs produce many peptides in a stress-dependent manner; this includes pro-enkephalin opioid gene products such as met-/leu-enkephalin[25–27]. We hypothesized that vesicular somatodendritic release of an opioid peptide is responsible for LTD_{GABA} following CORT exposure. In CORT-treated slices, continuous bath application of the broad-spectrum opioid receptor (OR) antagonist naloxone (5 μM) prevented pairing induced depression of eIPSC amplitude (100.7 ± 7.9% baseline; P = 0.93; Fig. 6a). Naloxone also prevented LTD_{GABA} associated changes to PPR (95.5 ± 4.4% baseline; P = 0.33), CV^{-2} (131.1 ± 16.4 %; P = 0.10), and sIPSC frequency (112.4 ± 13.3%; P = 0.38). Similarly, the μOR subtype antagonist CTAP (1 μM) prevented LTD_{GABA} (99.0 ± 9.3% baseline; P = 0.92; Fig. 6b). Neither the δOR antagonist (Naltrindole; 1 μM) nor the κORs antagonist (nor-Binaltorphimine; 1 μM) prevented LTD_{GABA} following pairing (71.1 ± 8.2 % and 71.5 ± 5.6 % baseline respectively; P = 0.017 and P = 0.0037; Supplementary Fig. 4c). We did, however, note suppressive effects of a κOR agonist U69593 (1 μM), but not δOR agonist DPDPE (1 μM) on eIPSC amplitude (U69593: 21.7 ± 7.6% baseline, P = 0.0005; DPDPE: 100.8 ± 5.8% baseline, P = 0.09; Supplementary

Fig. 4a–b). These pharmacological data suggest that μ-ORs are necessary for induction of LTD_{GABA} following CORT exposure. Finally, we assessed LTD in $\mu OR^{-/-}$ mice,[28]. We failed to observe any lasting depression of eIPSCs (106.4 ± 9.3 % baseline; P = 0.52; Fig. 6c). These data confirm that μORs are necessary for LTD_{GABA}.

μOR subtypes are commonly located on GABA neurons and their synaptic terminals[29–31]. If an endogenous opioid were released from PNCs, its actions would likely be spatially restricted to local terminals, particularly since cell bodies of afferent GABA neurons reside outside the PVN[4]. In line with this hypothesis, we found that DAMGO (1 μM) significantly reduced the frequency of miniature IPSCs (1 μM TTX; from 2.1 ± 0.6 to 0.7 ± 0.2 events · sec^{-1}; P = 0.0002 paired t-test; Fig. 6d) but not their amplitude (21.6 ± 1.1 pA before, 21.6 ± 0.7 pA after; P = 0.99), suggesting that μORs on terminals contacting PNCs regulate GABA p_r. Next we asked whether activation of presynaptically-located μORs would occlude the induction/expression of LTD. In CORT-treated cells, DAMGO (500 nM) depressed eIPSC amplitude (48.4 ± 8.4% baseline; PPR to 136.1 ± 11.5%; Fig. 6e). Once eIPSC amplitude had stabilized, we delivered the pairing protocol. This had no additional effect on either eIPSC amplitude or PPR. At 25 min after pairing, eIPSC amplitude was 52.8 ± 4.5% of pre-DAMGO baseline (paired t-test P = 0.48 vs. pre-DAMGO) and PPR: 133.8 ± 9.8% (paired t-test P = 0.89). We failed to observe significant changes to PNC holding current during DAMGO treatment (pooled 500 nM − 1 μM DAMGO; I_{hold} before: −17.3 ± 2.1 pA, after: −13.7 ± 2.7 pA; n = 27; paired t-test P = 0.13; not shown). Taken together these results demonstrate that μORs located at synaptic terminals suppress GABA release, and that their activation by an exogenous ligand occludes subsequent induction of LTD_{GABA}.

Although necessary for LTD_{GABA} expression, it is not clear whether μOR activation is necessary for its maintenance. We applied OR antagonist/inverse agonist naloxone (5 μM) 20 min following either DAMGO or induction of LTD_{GABA} by the pairing protocol. Transient μOR activation by DAMGO (1 μM, 7 min) caused a long-lasting depression of eIPSCs (65.6 ± 9.0 % baseline at 35 min; P = 0.0088; Fig. 7a). This depression was completely reversed by naloxone (111.7 ± 14.1 % baseline at 35 min; P = 0.44; Fig. 7a). These results, suggest that transient μOR activation is capable of eliciting a long-lasting synaptic change, that requires persistent OR signaling. Next, following pairing, we established that eIPSC amplitude was suppressed (60.9 ± 10.4 % baseline; P = 0.0093; Fig. 7b). Subsequent application of naloxone caused a recovery of eIPSCs to near-baseline level (108.5 ± 12.9 % baseline at 35 min; P = 0.53; Fig. 7a–b). PPR also returned to baseline (146.1 ± 16.8 % at 20 min; P = 0.033; to 106.4 ± 7.3 % at 35 min; P = 0.42; Fig. 7b). This was not due to pre-existing OR tone as naloxone application to CORT-treated PNCs (in the absence of pairing) had no effect on eIPSC amplitude (108.0 ± 4.0 % baseline; n = 5; P = 0.12; data not shown). In summary, LTD_{GABA} requires the μOR for both expression and maintenance of suppressed GABA release. This could be due to either persistent effects of μOR activation and/or sustained vesicular release of the opioid peptide.

LTD_{GABA} does not display synapse specificity

Opioid release and signaling may occur across the entire somatodendritic axis, or alternatively at locally recruited segments of the dendrite. Furthermore, presynaptic activity

or μOR expression could be restricted to certain inputs. Thus we probed whether LTD_{GABA} exhibited synapse specificity. Given that mIPSC frequency is sensitive to the μOR agonist DAMGO and that sIPSCs are also suppressed during LTD_{GABA}, we hypothesized that release, spread, and/or efficacy of endogenously release opioids would not be limited to synapses active during pairing. To test this, we electrically activated two distinct GABAergic inputs onto PNCs, s_1 and s_2, verifying their independence by confirming that the synaptic strength and release probability of one pathway was unaffected by recruiting the other pathway. Delivering the 10Hz stimulation during pairing through s_1, depressed eIPSC amplitude at both s_1 and s_2 inputs (s_1: 64.7 ± 4.4% baseline, s_2: 71.8 ± 10.2% baseline; P = 0.005 and P = 0.039 respectively; Fig. 8a).

Finally, given this finding and with demonstrations that GABA and glutamate synapses on PNCs are intermingled[32], we hypothesized that somatodendritically released opioids may also depress glutamate synapses. First, we tested for the presence of functional μORs at glutamate synapses. In slices incubated *in vitro* with CORT, evoked excitatory post-synaptic currents (eEPSCs) were suppressed by DAMGO (40.8 ± 6.2% baseline; P < 0.0001; Supplementary Fig. 4d). Next, we applied the pairing protocol used above and observed a long-lasting depression of glutamate transmission. eEPSC amplitude at 30 min was suppressed to 62.3 ± 9.4% baseline (P = 0.0073; Fig. 8b), which was accompanied by an increased PPR (125.6 ± 6.6% baseline; P = 0.0081) and a decrease in CV^{-2} (57.0 ± 15.0% baseline; P = 0.028), suggesting a presynaptic locus of expression. Naloxone completely prevented expression of LTD (102.4 ± 9.0% baseline; P = 0.802; Fig. 8b), changes in PPR (100.2 ± 9.9% baseline; P = 0.99) and changes in CV^{-2} (92.8 ± 12.6% baseline; P = 0.59). These results demonstrate that LTD mediated by ORs in PNCs following GC exposure occurs in a synapse-independent fashion.

Discussion

Here we show that glucocorticoids, elevated in response to a stress experience, are instructive signals in the hypothalamus that allow for subsequent correlated synaptic and cellular activity to suppress GABA p_r. By suppressing RGS4 in PNCs, glucocorticoids functionally alter the outcome of post-synaptic mGluR signaling during synaptic stimulation culminating in calcium-dependent vesicle exocytosis and the liberation of a retrograde opioid signal from the somatodendritic compartment. Activation of presynaptic μORs is necessary for the expression and maintenance of decreased neurotransmitter release, implicating an endogenous opioid as the most likely candidate for this retrograde signal.

Glucocorticoid-associated LTD_{GABA} requires heterosynaptic recruitment of $mGLuR_5$ located on PNCs themselves. This finding is consistent with reports of enhanced $mGluR_{1/5}$ signaling following stress/CORT exposure[33]. Importantly, pairing of afferent stimulation with a postsynaptic depolarization was necessary for LTD_{GABA} suggesting that G_q-linked mGluRs in our system may behave as voltage-dependent “coincidence detectors”[34,35]. Membrane depolarization has been shown to amplify mGluR signaling by enhancing contributions of voltage-gated calcium channels[36] which can synergize with and sustain calcium sourced by mGluRs from IP_3-receptor gated stores[34]. Although the mechanisms regulating somatodendritic exocytosis are not well defined[23], neuronal activity and G_q-

coupled receptors cooperatively drive calcium-dependent dendritic peptide release[37]. For example, synaptic mGluR activation during burst firing in MNCs[27] and L-type channels in dentate granule cells play important roles in dendritic release of the opioid dynorphin[24,38]. In accordance with these previous studies, our findings indicate that calcium entry through L-type voltage-gated calcium channels is obligatory for LTD_{GABA}. While somatodendritic vesicular release from PNCs can also occur following calcium influx through NMDARs[19], we found that LTD_{GABA} persisted after NMDAR blockade.

Our data suggest that μOR activation is necessary for expression of LTD_{GABA}. Intriguingly, we also found that ongoing OR activation is required for LTD maintenance, which is unconventional as an expression mechanism for long-term plasticity. μORs are functionally expressed within the PVN, and influence PNC activity and HPA function in a stress-state dependent manner[10,39,40]. In other brain regions μORs are widely expressed on GABAergic neurons and terminals[31]. μOR agonists hyperpolarize inhibitory neurons[29–31] and interfere with inhibitory synapse plasticity[41]. Agonist activation of μORs locally expressed at synaptic terminals also suppresses GABA p_r[42] and can induce LTD at both GABA and glutamate synapses[43,44]. In spite of this, there are only a few demonstrations of functional synaptic actions of endogenously produced and retrograde acting opioids[11,12]. One might conjecture that a likely candidate for the endogenous μOR ligand produced by PNCs and mediating LTD_{GABA} is an enkephalin-like peptide. PNC enkephalins are a compelling candidate for experience-dependent control of neuroendocrine function and adaptation. Proenkephalin transcripts are incrementally upregulated by acute and repeated stress[45] in a glucocorticoid-dependent manner[46,47]. Notably, proenkephalin is also increasingly colocalized with c-fos and/or CRH following stressful conditions[9,48], suggesting that enkephalin-containing neurons may be relevant to stress-related PNC plasticity, and that enkephalin-derived peptides may exist in PNCs as adaptogenic signaling molecules.

Although LTD_{GABA} reported here is not mediated by eCBs, it shares many similarities with eCB-LTD, which also occurs at synapses throughout the brain[16,18]. G_q-coupled metabotropic receptor activation is a strong stimulus for eCB production, and required for eCB-LTD[14–16,18]. Additionally, glucocorticoids enhance both eCB-mediated short- and long-term plasticity at GABA synapses[7,49]. We found that the switch in mGluR signaling necessary for LTD_{GABA} following CORT exposure is likely RGS4, a molecule which has recently been shown to regulate eCB-LTD through gating mGluR signaling in the striatum[50]. Despite these common features, our experiments indicate that LTD_{GABA} occurs independently of CB1Rs and, to our knowledge, is the first demonstration of an eCB-independent presynaptic LTD at mature GABAergic synapses.

PNC activity is known to be a function of both synaptic drive and circulating glucocorticoid levels. The CORT actions we observe here emerge within the time period classically defined as the “delayed” domain of glucocorticoid feedback[3]. During this time, endocrine responses to any subsequent stressors are blunted in proportion to the levels of CORT produced by the first exposure[3]. This period conforms with the time estimated for both the entry of CORT into the brain[13] and slow emergence of genomic glucocorticoid receptor-dependent actions[3]. Since GABA transmission onto PNCs during stress is excitatory[5,8], we propose that a retrograde opioid suppression of both GABA and glutamate release during a sustained

period of PNC activity represents a synaptic correlate of the glucocorticoid-induced "refractory period" imposed onto PNCs[3]. This mechanism may act to mask or compete with the "priming" mechanisms imparted to PNCs during a stress[3,19]. One such mechanism, set in place by the metaplastic actions of the other major stress mediator noradrenaline, is detailed in the accompanying study by Inoue et al. Our findings, together, provide mechanistic underpinnings for bidirectional synaptic adaptations that can occur during different temporal windows after a single stress experience. We observed that these two forms of plasticity also exhibit different thresholds for induction. For example, unlike LTP_{GABA} reported here at 0 min after stress, and extensively detailed by Inoue et al, LTD_{GABA} was only evident following a relatively longer period of sustained synaptic and postsynaptic activity. While speculative, given the paucity of data regarding firing patterns of PNCs or their afferents during *in vivo* stress, this induction requirement suggests LTD_{GABA} may preferentially serve a homeostatic function, imposing a ceiling on HPA activation and limiting systemic exposure to pathological levels of glucocorticoids during prolonged periods of stress. Together, our two studies suggest that polarity of synaptic metaplasticity on PNCs is a function of the time domain over which the body's two principal stress mediators elicit their actions, and hint at the complex dynamics that allow stress circuits to respond and evolve with experience.

Methods

Animal handling and stress procedure

All protocols were approved by the University of Calgary Animal Care & Use Committee, in accordance with the Canadian Council for Animal Care. Group-housed juvenile male Sprague Dawley rats (postnatal day 22–31, Charles Rivers), wild-type C57BL6/J (Jackson Laboratories), $\mu OR^{-/-}$ (Jackson Stock #007559), *vGAT–mhChR2–YFP* BAC transgenic (Jackson Stock #014548), or $CB1R^{-/-}$ (From Dr. K. Sharkey) mice (bred to C57BL6/J background, postnatal day 28–50) were kept on a 12:12 light dark cycle with ad libitum access to food and water. Stress was carried out 2–3 hours after the onset of light during the trough of circadian fluctuation in plasma CORT. Immobilization stress consisted of cervical and caudal immobilization and confinement within a plastic cylinder for 30 min. Forced swim stress was carried out for 20 min in a plastic bucket (40 cm internal diameter) and 30–32 °C water at a depth where the bottom could not be touched by the rat. To expose rats to predator odor they were placed in an empty cage for 30 min with a tissue soaked with 2,5-dihydro-2,4,5-trimethylthiazoline (TMT, Contech), a compound isolated from fox feces[19]. In some experiments, an intraperitoneal injection of RU-486 (25 $mg{\cdot}kg^{-1}$) or DMSO vehicle preceded stress by 15 min. Following stress, the rat was placed alone, in a fresh cage, until slice preparation.

Slice preparation and electrophysiology

Animals were anesthetized with isoflurane and decapitated. The brain was quickly removed; it was submerged and coronally sectioned on a vibratome (Leica) to 300 μM in slicing solution (0°C, 95% O_2/5% CO_2 saturated) containing (in mM): 87 NaCl, 2.5 KCl, 0.5 $CaCl_2$, 7 $MgCl_2$, 25 $NaHCO_3$, 25 D-glucose, 1.25 NaH_2PO_4, 75 sucrose. After placement into aCSF (30 °C, 95% O_2/5% CO_2 saturated) containing (in mM):126 NaCl, 2.5 KCl, 26

$NaHCO_3$, 2.5 $CaCl_2$, 1.5 $MgCl_2$, 1.25 NaH_2PO_4, 10 glucose, hypothalamic slices recovered for at least 1 hour. Subsequently, some slices were placed for 1 hour into aCSF containing 100 nM corticosterone and/or 500 nM RU-486 (Sigma; final DMSO vehicle: < 0.0001%). Once transferred to a recording chamber superfused with aCSF (1 $mL \cdot min^{-1}$; 30–32 °C; 95% O_2/5% CO_2), slices were visualized using an AxioskopII FS Plus (Zeiss) upright microscope fitted with infrared differential interference contrast optics. Pulled borosilicate glass pipettes (3–6 MΩ) were filled with a solution containing (in mM) 108 K-gluconate, 2 $MgCl_2$, 8 Na-gluconate, 8 KCl, 1 K_2-EGTA, 4 K_2-ATP, 0.3 Na_3-GTP, and 10 mM HEPES. In indicated experiments KCl was reduced to 4 mM or the following were added: 10 mM 1,2-Bis(2-aminophenoxy)ethane-N,N,N′,N′-tetraacetic acid (BAPTA; Sigma), 5 $\mu g \cdot mL^{-1}$ Botulinum Neurotoxin Type C (Light Chain Recombinant BoNT/C; List Biological), 1mM (+)-5-methyl-10,11-dihydro-5H-dibenzo[a,d]cyclohepten-5,10-imine maleate (MK801), 2 mM GDPβs (Na_3GTP-free solution), CCG63802 (Tocris), or recombinant RGS4 (Genway). All other drugs were bath applied by perfusion pump. MCPG, MTEP, JNJ 16259685, capsazepine, and DHPG were obtained from Tocris, [D-$Pen^{2,5}$] Enkephalin, [D-Pen^2,D-Pen^5]Enkephalin (DPDPE) was from Bachem, and nimodipine. Picrotoxin, U69593, [D-Ala^2, NMe-Phe^4, Gly-ol^5]-enkephalin (DAMGO), CTAP, naltrindole, and naloxone were from Sigma.

Whole-cell patch-clamp recordings were performed from PNCs identified by location, morphology, and current clamp fingerprint, as previously described[5,7,19]. Of the 2–4 PVN slices obtained from each animal, one cell was recorded per slice. Slices were randomly assigned to treatment/no-treatment groups; a minimum of 2 cells per litter were used as no-treatment control. Each group consists of data obtained from at a minimum 3 animals from 2 different litters. Sample sizes were determined *post-hoc* based on those used in previous studies[5,7,19]. Experimenters were not blinded to treatment. PNCs were voltage-clamped at −80 mV with constant perfusion of 6,7-dinitroquinoxaline-2,3-dione (DNQX; 10 μM; Tocris) or picrotoxin (100 μM; Sigma). Pairs of post-synaptic currents (IPSCs) were evoked 50 milliseconds apart at 0.2 Hz intervals using a monopolar aCSF-filled glass electrode placed about 25 to 50 μm ventromedially from the recorded cell. To activate ChR2, a fiber optic cable (105 μm core diameter) was placed 1–2 mm from the PVN and a blue-light laser (473 nm, OptoGeni 473, IkeCool corporation) delivered 3–5 millisecond light pulses at 0.2Hz. The protocol used to elicit LTD consisted of 10 Hz synaptic stimulation paired with a voltage-clamp step to −40 mV for 5 min. Access resistance was continuously monitored; recordings in which values exceeded 20 MΩ or 15% change were excluded from analysis.

Data analysis and statistics

Signals were amplified (Multiclamp 700B, Molecular Devices), low pass filtered at 1 kHz, digitized at 10 kHz (Digidata 1322, Molecular Devices), and recorded (pClamp 9.2, Molecular Devices) for offline analysis. PSC amplitudes were calculated by subtraction of peak synaptic current from pre-stimulation baseline current. sIPSC events, with eIPSCs and stimulus artifacts removed, were detected using variable thresholds and confirmed by eye (MiniAnalysis, Synaptosoft). For each cell, mean eIPSC/eEPSC amplitude, paired-pulse ratio (2^{nd} evoke/1^{st} evoke), or sIPSC event frequency/amplitude obtained over a 2-min recording interval were normalized and expressed as a percent of baseline recording values.

Coefficient of variation (CV^{-2}) was analyzed with a 5-min interval, and expressed as percent baseline. Gaussian distribution of the data was confirmed by a D'Agostino & Pearson omnibus normality test (GraphPad Prism 4). A one-sample t-test (vs. 100%) was used to assess deviation in normalized values from baseline, and a paired two-tailed student's t-test (where stated) to assess deviation in non-normalized values. $P < 0.05$ was considered the level of statistical significance.

Supplementary Material

Refer to Web version on PubMed Central for supplementary material.

Acknowledgments

We acknowledge Bains lab members for thoughtful discussion and Cheryl Sank and Robert Cantrup for technical assistance. We thank Drs. Quentin Pittman and Karl Iremonger for helpful comments on the manuscript and Dr. Keith Sharkey for providing $CB1^{-/-}$ mice. We thank the Hotchkiss Brain Institute (HBI) support of the optogenetics core. J.S.B is a Alberta Innovates for Health Solutions (AI-HS) Senior Scholar. This work was supported by an operating grant from the Canadian Institutes of Health Research MOP 86501 to J.S.B. W.I. and T.F are supported by postdoctoral fellowships, and J.I.W by a PhD scholarship from AI-HS. W.I. and J.I.W. also received fellowship/scholarship support from the HBI.

References

1. de Kloet ER, Joëls M, Holsboer F. Stress and the brain: from adaptation to disease. Nat Rev Neurosci. 2005; 6:463–475. [PubMed: 15891777]
2. Joels M, Baram TZ. The neuro-symphony of stress. Nat Rev Neurosci. 2009; 10:459–466. [PubMed: 19339973]
3. Keller-Wood ME, Dallman MF. Corticosteroid inhibition of ACTH secretion. Endocrine Reviews. 1984; 5:1–24. [PubMed: 6323158]
4. Miklós IH, Kovács KJ. GABAergic innervation of corticotropin-releasing hormone (CRH)-secreting parvocellular neurons and its plasticity as demonstrated by quantitative immunoelectron microscopy. Neuroscience. 2002; 113:581–592. [PubMed: 12150778]
5. Hewitt SA, Wamsteeker JI, Kurz EU, Bains JS. Altered chloride homeostasis removes synaptic inhibitory constraint of the stress axis. Nat Neurosci. 2009; 12:438–443. [PubMed: 19252497]
6. Verkuyl J, Karst H, Joëls M. GABAergic transmission in the rat paraventricular nucleus of the hypothalamus is suppressed by corticosterone and stress. Eur J Neurosci. 2005; 21:113–121. [PubMed: 15654848]
7. Wamsteeker JI, Kuzmiski JB, Bains JS. Repeated Stress Impairs Endocannabinoid Signaling in the Paraventricular Nucleus of the Hypothalamus. J Neurosci. 2010; 30:11188–11196. [PubMed: 20720126]
8. Sarkar J, Wakefield S, MacKenzie G, Moss SJ, Maguire J. Neurosteroidogenesis Is Required for the Physiological Response to Stress: Role of Neurosteroid-Sensitive GABAA Receptors. J Neurosci. 2011; 31:18198–18210. [PubMed: 22171026]
9. Watts AG. Glucocorticoid regulation of peptide genes in neuroendocrine CRH neurons: a complexity beyond negative feedback. Front Neuroendocrinol. 2005; 26:109–130. [PubMed: 16289311]
10. Bilkei-Gorzo A, et al. Control of hormonal stress reactivity by the endogenous opioid system. Psychoneuroendocrinology. 2008; 33:425–436. [PubMed: 18280051]
11. Iremonger KJ, Bains JS. Retrograde Opioid Signaling Regulates Glutamatergic Transmission in the Hypothalamus. J Neurosci. 2009; 29:7349–7358. [PubMed: 19494156]
12. Wagner JJ, Terman GW, Chavkin C. Endogenous dynorphins inhibit excitatory neurotransmission and block LTP induction in the hippocampus. Nature. 1993; 363:451–454. [PubMed: 8099201]

13. Droste SK, et al. Corticosterone Levels in the Brain Show a Distinct Ultradian Rhythm but a Delayed Response to Forced Swim Stress. Endocrinology. 2008; 149:3244–3253. [PubMed: 18356272]
14. Ronesi J, Lovinger DM. Induction of striatal long-term synaptic depression by moderate frequency activation of cortical afferents in rat. J Physiol. 2005; 562:245–256. [PubMed: 15498813]
15. Puente N, et al. Polymodal activation of the endocannabinoid system in the extended amygdala. Nat Neurosci. 2011; 14:1542–1547. [PubMed: 22057189]
16. Castillo PE, Chiu CQ, Carroll RC. Long-term plasticity at inhibitory synapses. Curr Opin Neurobiol. 2011; 21:328–338. [PubMed: 21334194]
17. Regehr WG, Carey MR, Best AR. Activity-dependent regulation of synapses by retrograde messengers. Neuron. 2009; 63:154–170. [PubMed: 19640475]
18. Chevaleyre V, Castillo PE. Heterosynaptic LTD of Hippocampal GABAergic Synapses: A Novel Role of Endocannabinoids in Regulating Excitability. Neuron. 2003; 38:461–472. [PubMed: 12741992]
19. Kuzmiski JB, Marty V, Baimoukhametova DV, Bains JS. Stress-induced priming of glutamate synapses unmasks associative short-term plasticity. Nat Neurosci. 2010; 13:1257–1264. [PubMed: 20818385]
20. Saugstad JA, Marino MJ, Folk JA, Hepler JR, Conn PJ. RGS4 inhibits signaling by group I metabotropic glutamate receptors. J Neurosci. 1998; 18:905–913. [PubMed: 9437012]
21. Ni YG, et al. Region-Specific Regulation of RGS4 (Regulator of G-Protein–Signaling Protein Type 4) in Brain by Stress and Glucocorticoids: In Vivo and In Vitro Studies. J Neurosci. 1999; 19:3674–3680. [PubMed: 10233999]
22. Kim G, et al. Acute stress responsive RGS proteins in the mouse brain. Mol Cells. 2010; 30:161–165. [PubMed: 20680490]
23. Ludwig M, Pittman QJ. Talking back: dendritic neurotransmitter release. Trends in Neurosciences. 2003; 26:255–261. [PubMed: 12744842]
24. Iremonger KJ, Kuzmiski JB, Baimoukhametova DV, Bains JS. Dual Regulation of Anterograde and Retrograde Transmission by Endocannabinoids. J Neurosci. 2011; 31:12011–12020. [PubMed: 21849561]
25. Ceccatelli S, Eriksson M, Hokfelt T. Distribution and coexistence of corticotropin-releasing factor-like, neurotensin-like, enkephalin-like, cholecystokinin-like, galanin-like and vasoactive intestinal polypeptide peptided histidine isoleucine-like peptides in the parvocellular part of the paraventricular nucleus. Neuroendocrinology. 1989; 49:309–323. [PubMed: 2469987]
26. Pretel S, Piekut D. Coexistence of corticotropin-releasing factor and enkephalin in the paraventricular nucleus of the rat. J Comp Neurol. 1990; 294:192–201. [PubMed: 2332527]
27. Merchenthaler I. Enkephalin-immunoreactive neurons in the parvicellular subdivisions of the paraventricular nucleus project to the external zone of the median eminence. J Comp Neurol. 1992; 326:112–120. [PubMed: 1479064]
28. Contet C, et al. Dissociation of Analgesic and Hormonal Responses to Forced Swim Stress Using Opioid Receptor Knockout Mice. Neuropsychopharmacology. 2005; 31:1733–1744. [PubMed: 16237385]
29. Nicoll RA, Alger BE, Jahr CE. Enkephalin blocks inhibitory pathways in the vertebrate CNS. Nature. 1980; 287:22–25. [PubMed: 6251377]
30. Zieglgansberger W, French E, Siggins G, Bloom F. Opioid peptides may excite hippocampal pyramidal neurons by inhibiting adjacent inhibitory interneurons. Science. 1979; 205:415–417. [PubMed: 451610]
31. Williams JT, Christie MJ, Manzoni O. Cellular and Synaptic Adaptations Mediating Opioid Dependence. Physiol Rev. 2001; 81:299–343. [PubMed: 11152760]
32. Decavel C, Van den Pol AM. Converging GABA- and Glutamate-Immunoreactive Axons Make Synaptic Contact With Identified Hypothalamic Neurosecretory Neurons. Journal of Comparative Neurology. 1992; 316:104–116. [PubMed: 1349310]
33. Chaouloff F, Hémar A, Manzoni O. Acute Stress Facilitates Hippocampal CA1 Metabotropic Glutamate Receptor-Dependent Long-Term Depression. J Neurosci. 2007; 27:7130–7135. [PubMed: 17611266]

34. Nakamura T, Barbara JG, Nakamura K, Ross WN. Synergistic Release of Ca2+ from IP3-Sensitive Stores Evoked by Synaptic Activation of mGluRs Paired with Backpropagating Action Potentials. Neuron. 1999; 24:727–737. [PubMed: 10595522]
35. Billups D, Billups B, Challiss RAJ, Nahorski SR. Modulation of Gq-Protein-Coupled Inositol Trisphosphate and Ca2+ Signaling by the Membrane Potential. J Neurosci. 2006; 26:9983–9995. [PubMed: 17005862]
36. Carter AG, Sabatini BL. State-dependent calcium signaling in dendritic spines of striatal medium spiny neurons. Neuron. 2004; 44:483–493. [PubMed: 15504328]
37. Ludwig M, et al. Intracellular calcium stores regulate activity-dependent neuropeptide release from dendrites. Nature. 2002; 418:85–89. [PubMed: 12097911]
38. Simmons ML, Terman GW, Gibbs SM, Chavkin C. L-type calcium channels mediate dynorphin neuropeptide release from dendrites but not axons of hippocampal granule cells. Neuron. 1995; 14:1265–1272. [PubMed: 7605635]
39. Buckingham JC. Secretion of Corticotrophin and Its Hypothalamic Releasing Factor in Response to Morphine and Opioid Peptides. Neuroendocrinology. 1982; 35:111–116. [PubMed: 6290921]
40. Kiritsy-Roy JA, Appel NM, Bobbitt FG, Van Loon GR. Effects of mu-opioid receptor stimulation in the hypothalamic paraventricular nucleus on basal and stress-induced catecholamine secretion and cardiovascular responses. J Pharmacol Exp Ther. 1986; 239:814–822. [PubMed: 3025420]
41. Nugent FS, Penick EC, Kauer JA. Opioids block long-term potentiation of inhibitory synapses. Nature. 2007; 446:1086–1090. [PubMed: 17460674]
42. Cohen GA, Doze VA, Madison DV. Opioid inhibition of GABA release from presynaptic terminals of rat hippocampal interneurons. Neuron. 1992; 9:325–335. [PubMed: 1497896]
43. Lafourcade CA, Alger BE. Distinctions among GABA(A) and GABA(B) responses revealed by calcium channel antagonists, cannabinoids, opioids, and synaptic plasticity in rat hippocampus. Psychopharmacology. 2008; 198:539–549. [PubMed: 18097653]
44. Yang YL, Atasoy D, Su HH, Sternson SM. Hunger States Switch a Flip-Flop Memory Circuit via a Synaptic AMPK-Dependent Positive Feedback Loop. Cell. 2011; 146:991–1002.
45. Larsen PJ, Mau SE. Effect of acute stress on the expression of hypothalamic messenger ribonucleic acids encoding the endogenous opioid precursors preproenkephalin A and proopiomelanocortin. Peptides. 1994; 15:783–790. [PubMed: 7984495]
46. Garcia -Garcia L, Harbuz MS, Manzanares J, Lightman SL, Fuentes JA. RU-486 blocks stress-induced enhancement of proenkephalin gene expression in the paraventricular nucleus of rat hypothalamus. Brain Res. 1998; 786:215–218. [PubMed: 9555022]
47. Lightman SL, Young WS. Influence of steroids on the hypothalamic corticotropin-releasing factor and preproenkephalin mRNA responses to stress. Proc Natl Acad Sci U S A. 1989; 86:4306–4310. [PubMed: 2786213]
48. Dumont EC, Kinkead R, Trottier JF, Gosselin I, Drolet G. Effect of Chronic Psychogenic Stress Exposure on Enkephalin Neuronal Activity and Expression in the Rat Hypothalamic Paraventricular Nucleus. J Neurochem. 2000; 75:2200–2211. [PubMed: 11032909]
49. Sumislawski JJ, Ramikie TS, Patel S. Reversible Gating of Endocannabinoid Plasticity in the Amygdala by Chronic Stress: A Potential Role for Monoacylglycerol Lipase Inhibition in the Prevention of Stress-Induced Behavioral Adaptation. Neuropsychopharmacology. 2011; 36:2750–2761. [PubMed: 21849983]
50. Lerner, Talia N., Kreitzer, Anatol C. RGS4 Is Required for Dopaminergic Control of Striatal LTD and Susceptibility to Parkinsonian Motor Deficits. Neuron. 2012; 73:347–359. [PubMed: 22284188]

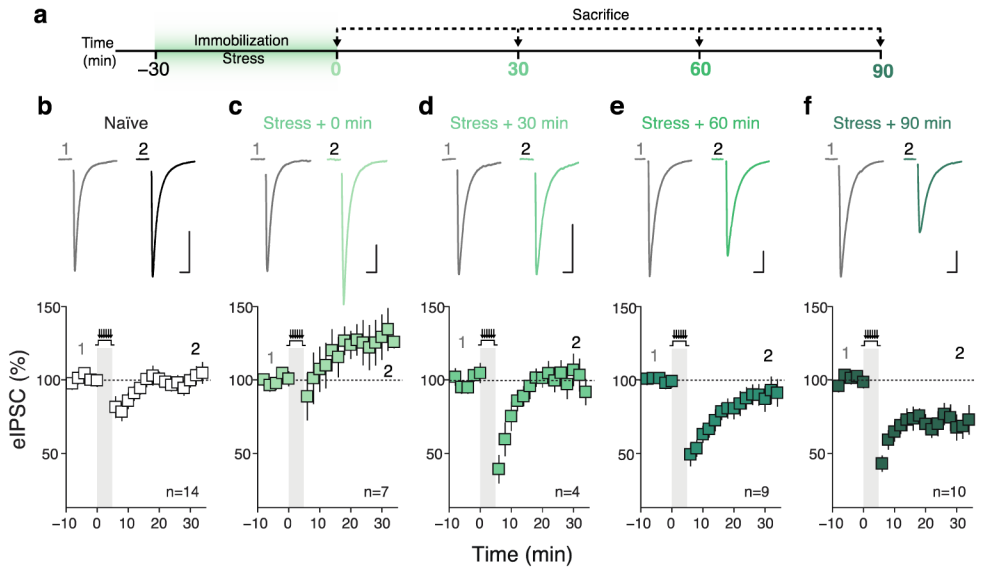

Figure 1. Stress unmasks long–term plasticity of GABA synapses

a) Overview of experimental paradigm. **b–f)** Above: sample traces of eIPSCs recorded from individual PNCs either before (1) or 30 min after (2) a pairing stimulation protocol consisting of 5 minutes of afferent stimulation (10 Hz) and postsynaptic depolarization (to −40 mV). Below: summary graphs for each treatment group show normalized eIPSC amplitudes before and after pairing (Naïve: n = 14 cells, 10 rats; Stress + 0 min: n = 7 cells, 4 rats; Stress + 30 min: n = 4 cells, 3 rats; Stress + 60 min: n = 9 cells, 4 rats; Stress + 90 min: n = 10 cells, 7 rats). Scale bars are 50 pA/10 ms. Data expressed as mean ± s.e.m.

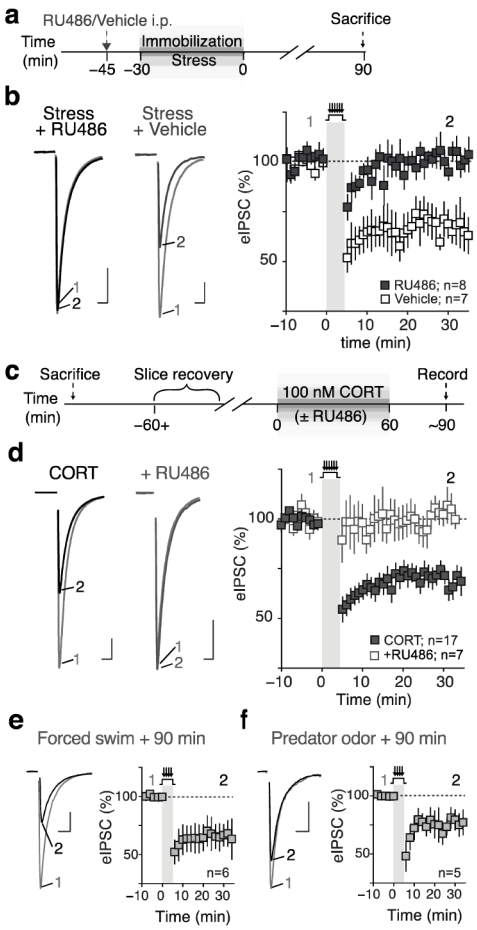

Figure 2. Glucocorticoid receptor activation is necessary and sufficient to unmask LTD_{GABA}

a) Overview of experimental paradigm in which either the glucocorticoid receptor antagonist RU-486 (25 mg · kg^{-1}) or vehicle were administered i.p. 15 min prior to stress. **b)** left: sample eIPSC traces from individual cells of stressed and RU-486− or stressed and vehicle-treated rats before and 30 min after pairing. Right: graph summarizes normalized eIPSC amplitudes in these groups (RU-486: n = 8 cells, 5 rats; vehicle: n = 7 cells, 3 rats). **c)** Overview of experimental paradigm in which hypothalamic slices from naïve rats were incubated in vitro with corticosterone (CORT; 100 nM) in the presence or absence of RU-486 (500 nM). **d)** left: sample eIPSC traces from individual cells of CORT− and CORT +RU-486- incubated slices before and 30 min after pairing. Right: graph summarizes normalized eIPSC amplitudes in these groups (CORT: n = 17 cells, 16 rats; CORT+RU-486: n = 7 cells, 4 rats). **e,f)** Left: sample eIPSC traces before and 30 min after pairing Right: Graphs summarizing normalized eIPSC amplitude in cells from rats exposed to forced swim (n = 6 cells, 3 rats) or predator odor (n = 5 cells, 5 rats) followed by a 90 min recovery period. Scale bars are 50 pA/10 ms. Data expressed as mean ± s.e.m.

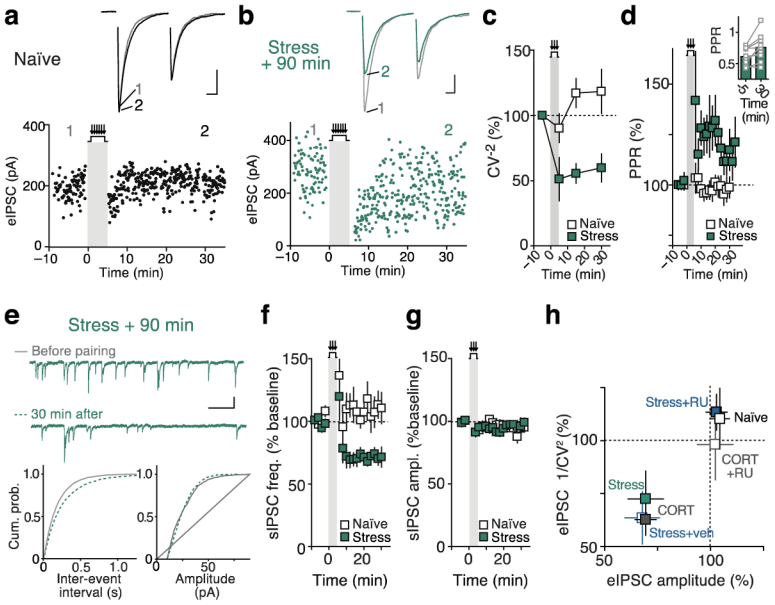

Figure 3. LTD$_{GABA}$ is expressed presynaptically

a–b) Sample paired-pulse traces and amplitude time courses of eIPSCs before and after pairing from individual cells in slices prepared from naïve or stressed rats. Scale bars are 50 pA/10 ms. **c–d)** Summary graphs of normalized eIPSC variability (CV^{-2}) and paired pulse-ratio (PPR) responses to the pairing protocol in cells from naïve (n = 14 cells, 10 rats) and stressed rats (n = 10 cells, 7 rats). **e)** Sample traces of sIPSCs and corresponding cumulative probability distribution plots of inter-event interval and amplitude before and 30 min following pairing in a cell from a stressed rat. Scale bars 20 pA/0.25 s. **f–g)** Summary graphs of normalized sIPSC frequency and amplitude response in naïve and stressed cells. **h)** Relationship between eIPSC amplitude and CV^{-2} changes at 30 min. Data expressed as mean ± s.e.m.

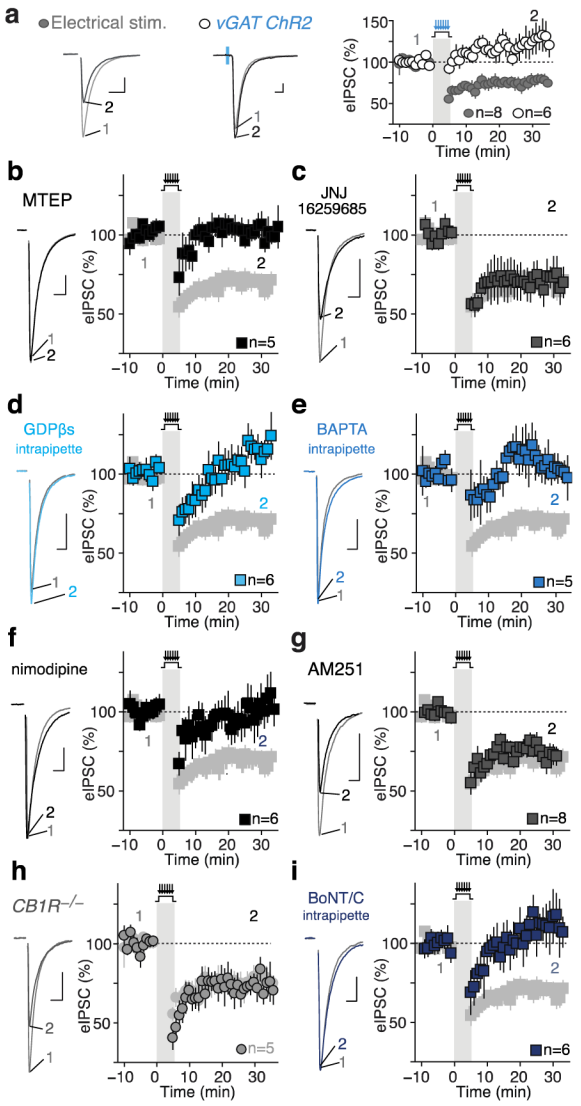

Figure 4. LTD_{GABA} induction is heterosynaptic and requires a retrograde signal

a) Response to pairing in CORT-treated slices with exclusive activation of GABA synapses in vGAT-ChR2 mice (open circles; n = 6 cells, 3 mice). Comparison with electrical stimulation in slices from WT mice (filled circles; n = 8 cells, 5 mice). Sample eIPSCs from individual PNCs are shown to the left and a summary graph to right. **b)** Effects of $mGluR_5$ antagonist MTEP (10μM; n = 5 cells, 3 rats) or **c)** $mGluR_1$ antagonist JNJ16259685 (750 nM; n = 6 cells, 5 rats) on LTD. Prevention of LTD_{GABA} by inclusion, in the patch pipette of: **d)** GTP-ase inhibitor GDPβs (2 mM; n = 6 cells, 3 rats), or e) calcium chelator, BAPTA (10 mM; n = 5 cells, 4 rats). **f)** Effect of bath application of the L-type calcium channel blocker nimodipine on LTD_{GABA} (20 μM; n = 6 cells, 4 rats). **g–h)** Effects of CB1R-antagonist AM251, in rats, or genetic deletion of the CB1R (*CB1R*$^{-/-}$), in mice, on LTD_{GABA} with eIPSC traces (left) and summary time course (right) (**g:** 3 μM; n = 8 cells, 5 rats or **h:** n = 5 cells, 3 mice). **i)** Prevention of LTD_{GABA} by intrapipette inclusion of SNARE-dependent exocytosis inhibitor BoNT/C (5μg · mL^{-1}; n = 6 cells, 3 rats). Control

LTD_{GABA} replotted in filled grey squares (rat) or circles (mouse). Scale bars are 50 pA/10 ms. Data expressed as mean ± s.e.m.

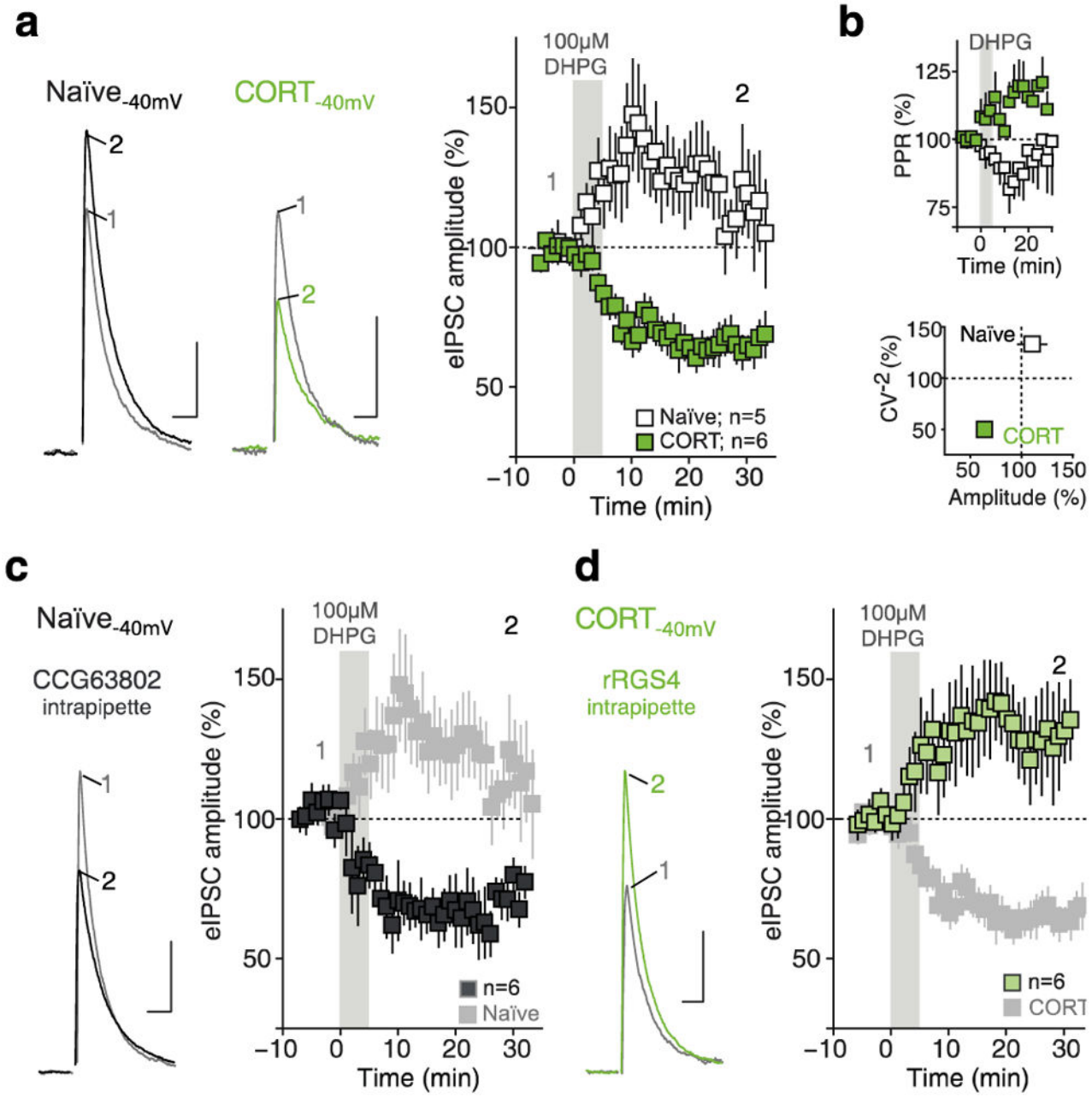

Figure 5. Glucocorticoid receptor activation modifies mGluR signaling via RGS4

a) Suppression of GABA transmission by mGluR agonist after glucocorticoid exposure. Left: sample eIPSC traces at a holding potential of −40 mV from individual naïve and CORT-treated cells before and 30 min after bath-applied $mGluR_{1/5}$ agonist DHPG (100 μM, 5 min). right: summary of the effects of DHPG on eIPSC amplitude at −40 mV in naïve (n = 5 cells, 3 rats) and CORT-treated (n = 6 cells, 4 rats) slices. **b)** Above: summary time course graph of normalized PPR in response to DHPG in naïve or CORT-treated slices. Below: relationship between eIPSC amplitude and CV^{-2} changes 30 min post-DHPG for each treatment group. **c)** mGluR supression of GABA transmission in naïve slices with inhibition

of post-synaptic RGS4. eIPSC traces from an individual cell (left) and summary data (right) from cells in a naïve slice treated with DHPG when the RGS4 inhibitor CCG63802 (100 μM) is included in the patch pipette (n = 6 cells, 4 rats). **d)** mGluR modulation of GABA transmission in CORT-treated slices with post-synaptic RGS4. eIPSC traces from an individual cell (left) and summary data (right) from cells of CORT-treated slices in which the pipette solution contained recombinant RGS4 (50 pM; n = 6 cells, 3 rats). Scale bars are 50 pA/10 ms. Data expressed as mean ± s.e.m.

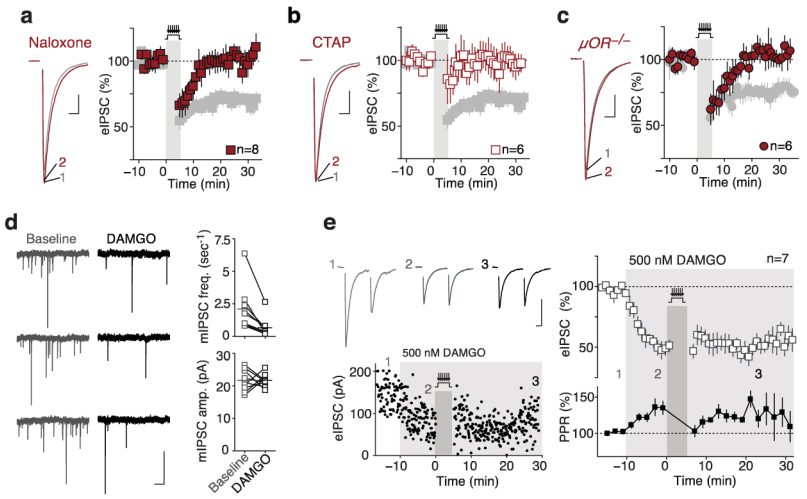

Figure 6. Presynaptic μ-type opioid receptors mediate LTD_{GABA}

a,b) Effect of μOR antagonism on LTD_{GABA}. eIPSC traces (left) and summary time course (right) showing the effects of pairing in CORT-treated slices in the presence of non-specific OR antagonist naloxone (5 μM; n = 8 cells, 5 rats) or μOR antagonist CTAP (1 μM, n = 6 cells, 4 rats). **c)** Effect of genetic deletion of μORs on LTD. eIPSC traces (left) and summary time course (right) shows the effects of pairing in CORT-treated slices from mice lacking μORs (n = 6 cells, 3 mice). **d)** Sample recording from an individual PNC (left) and summary graphs (right) of the frequency and amplitude of mIPSCs recorded in TTX (1 μM) showing the reduction of mIPSC frequency elicited by μOR agonist DAMGO (1 μM; n = 9 cells, 7 rats). **e)** Occlusion of LTD by μOR agonist DAMGO. eIPSC traces (above left) and eIPSC amplitude time course (below left) from a single neuron (CORT-treated) during baseline recording, following bath perfusion of μOR agonist DAMGO (500 nM), and 25 min after pairing. Summarized time course graph (right) showing the effects of pairing on normalized eIPSC amplitude (above) and PPR (below; n = 7 cells, 4 rats) following DAMGO treatment. Control LTD_{GABA} re-plotted in filled grey squares (rat) or circles (mouse). Scale bars are 50 pA/10ms in **a–d, g** and 25 pA/0.5 s in **e.** data expressed as mean ± s.e.m.

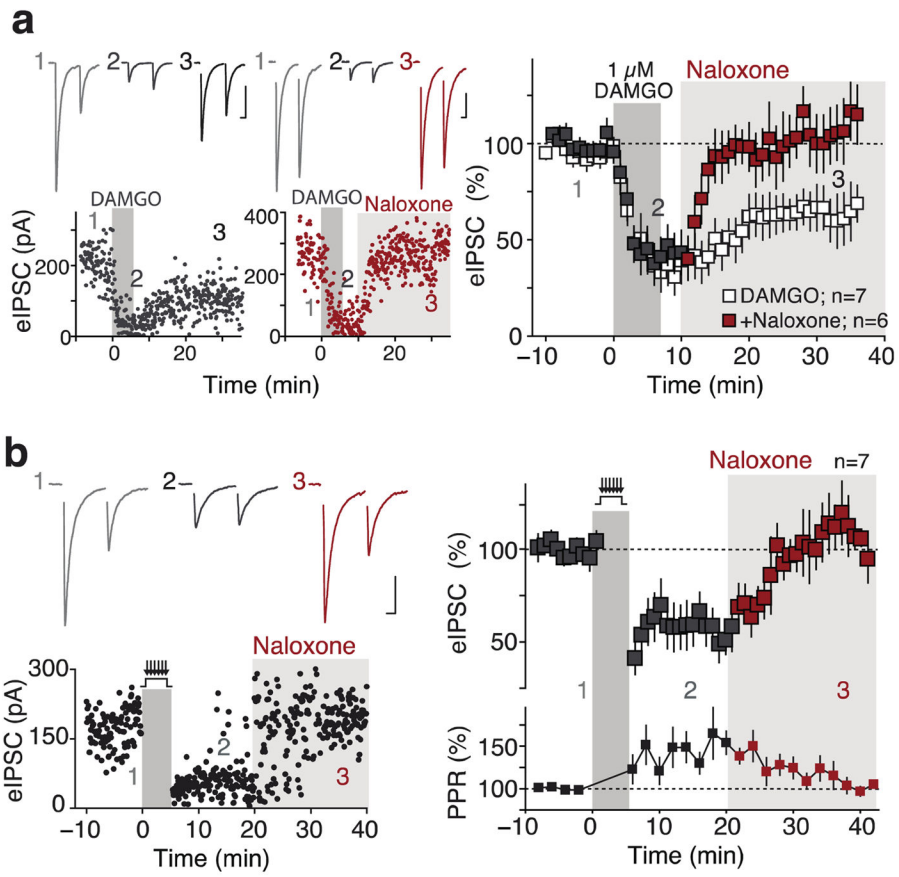

Figure 7. LTD_{GABA} is reversible by OR antagonism

a) Reversal of μOR agonist suppressed transmission by OR antagonist chase. Left: Sample eIPSC traces and right: plot of eIPSC amplitudes from a neuron treated with 1 μM DAMGO for 7 min (above) and another neuron with DAMGO treatment followed by naloxone (5 μM) at 10 min (below). Summary graph (right) showing effects of DAMGO on eIPSC amplitude alone (n = 7 cells, 6 rats) or followed by naloxone (n = 6 cells, 5 rats). **b)** Reversal of LTD by an OR antagonist. Sample eIPSC traces (above) and plot of eIPSC amplitude (below) taken from an individual cell in CORT-treated slices subjected to pairing followed by naloxone 20 min later. Right: Summary of the effects of naloxone (5 μM) applied following induction of CORT-LTD on eIPSC amplitude (above) and PPR (below) from n = 7 cells, 6 rats. Scale bars are 50 pA/10 ms. Data expressed as mean ± s.e.m.

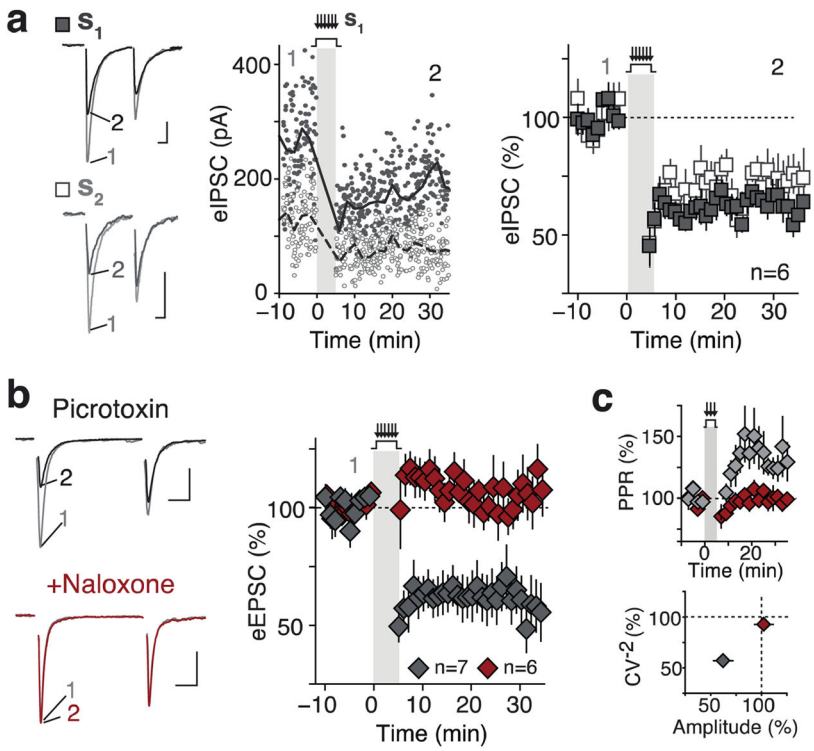

Figure 8. LTD_{GABA} is not synapse specific

a) Left: a schematic of experiment in which one PNC is recorded and two independent synaptic inputs (S1 and S2) onto the cell are stimulated. Only S1 is activated during the pairing protocol. eIPSC traces and eIPSC amplitude graph (center) from two inputs onto a single neuron before and after pairing. Right: summary data from this experiment shows pairing-induced depression of eIPSC amplitude of S1 and S2 (n = 6 cells, 4 rats). **b–c)** OR-mediated CORT-LTD at excitatory synapses. b) Left: eEPSC traces isolated by picrotoxin (100 μM) before and 30 min after pairing in a cell from a CORT-incubated slice (above) and a cell recorded in the presence of naloxone (below). Right: Summary time course of the effects of pairing on eEPSC amplitude with (n = 6 cells, 5 rats) or without naloxone (n = 7 cells, 5 rats). **c)** plot of normalized PPR response to pairing (above) and relationship between eEPSC and CV^{-2} (below) in CORT-treated cells with or without naloxone. Scale bars are 50 pA/10 ms. Data expressed as mean ± s.e.m.